

SCIENTIFIC REPORTS



OPEN

Singular observation of the polarization-conversion effect for a gammadion-shaped metasurface

Chu-En Lin¹, Ta-Jen Yen², Chih-Jen Yu³, Cheng-Min Hsieh³, Min-Han Lee², Chii-Chang Chen⁴ & Cheng-Wei Chang²

Received: 13 October 2015

Accepted: 09 February 2016

Published: 26 February 2016

In this article, the polarization-conversion effects of a gammadion-shaped metasurface in transmission and reflection modes are discussed. In our experiment, the polarization-conversion effect of a gammadion-shaped metasurface is investigated because of the contribution of the phase and amplitude anisotropies. According to our experimental and simulated results, the polarization property of the first-order transmitted diffraction is dominated by linear anisotropy and has weak depolarization; the first-order reflected diffraction exhibits both linear and circular anisotropies and has stronger depolarization than the transmission mode. These results are different from previously published research. The Mueller matrix ellipsometer and polar decomposition method will aid in the investigation of the polarization properties of other nanostructures.

In recent years, there have been demands for miniature optical devices that are thinner, lighter and more efficient^{1–3}. Thus, some chiral nanostructures were proposed for significant phenomena in polarization conversion. Gammadion-shaped metasurfaces have been discussed extensively because they are potential devices for optical applications. According to the previous research, the polarization conversion is caused by circular birefringence (CB) because of the asymmetric structures^{4,5}. In 2003, Papakostas *et al.* proposed an asymmetric gammadion-shaped structure that could rotate incident linearly polarized light at an angle. They claimed that the phenomenon resulted from optical activity⁵. In 2012, a review article by Li *et al.* also concluded that some asymmetric nanostructures could rotate the incident polarization state with CB⁶. However, the phenomenon of optical rotation results from CB, linear birefringence (LB), and linear diattenuation (LD), for example, LB, such as a half-wave plate, CB, such as a quartz crystal or glucose water solution, and linear diattenuation, such as a linear polarizer, can change the azimuth angle of incident polarized light^{7–9}. Additionally, the change in the ellipticity angle results from the contributions of circular diattenuation (CD) and LB. A polarimetric method that completely characterizes the polarization conversion mechanism of the gammadion-shaped metasurfaces will aid our understanding of the mechanism of the optical-rotation phenomena. To clearly describe the polarization transfer function of the gammadion-shaped metasurface, in 1943, Hans Mueller proposed the idea of Mueller calculus to study the relationships among the polarization effect of input light, output light, and materials¹⁰. Thus, the Mueller matrix can be used to determine the polarization properties of a material and predict the polarization state of the output light. Furthermore, Owing to the measured Mueller matrix, this matrix can be decomposed to analyze the three polarization properties of depolarization, diattenuation, and retardation according to the polar decomposition^{11–13}. Unlike the well-known Jones calculus¹⁴, Mueller calculus provides more information, such as unpolarized light, partially polarized light, and depolarization.

In this study, the Mueller matrix ellipsometer was used to investigate and analyze the polarization-conversion mechanism of gammadion-shaped nanostructures. The polarization-conversion effect did not result from CB only, which is in contrast to previous research^{5,6}. The experimental outcome indicates that the optical-rotation phenomenon of transmitted light of first-order diffraction is dominated by LD and that the change of ellipticity angle is dominated by LB. Additionally, for the reflection case, the optical-rotation phenomenon of reflected light

¹Department of Mechanical Engineering, National Chin-Yi University of Technology, Taichung 411, Taiwan.

²Department of Material Science and Engineering, National Tsing Hua University 300 Hsinchu, Taiwan. ³Graduate Institute of Electro-Optical Engineering, Chang Gung University 333 Taoyuan, Taiwan. ⁴Department of Optics and Photonics, National Central University 320 Taoyuan, Taiwan. Correspondence and requests for materials should be addressed to C.-J.Y. (email: cju@mail.cgu.edu.tw)

Parameter Names	Parameter		
	Linewidth (nm)	Number of branches	Metal thickness (nm)
G215	100	2	50
G218	100	2	80
G315	100	3	50

Table 1. Physical parameters of the fabricated samples.

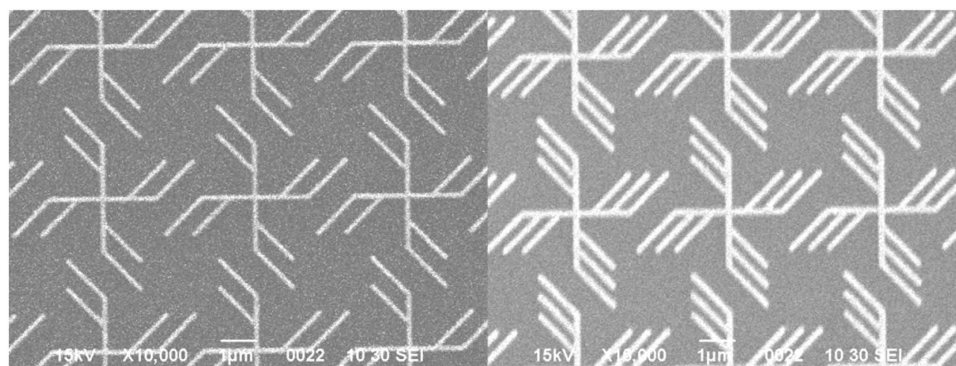


Figure 1. (a) SEM image of the two-branch structure. (b) SEM image of the three-branch structure.

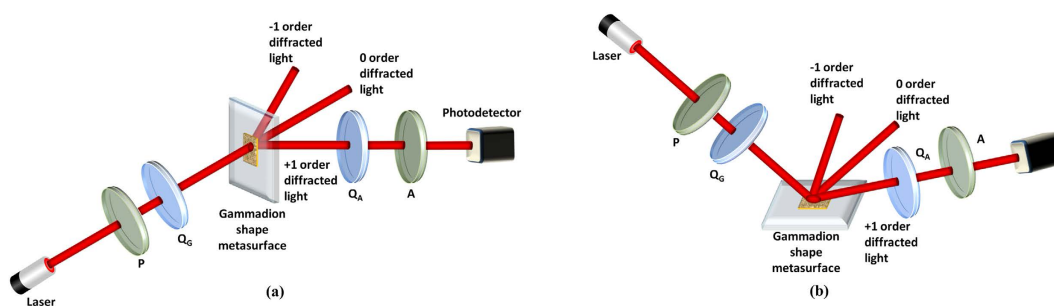


Figure 2. Experimental setup of the Mueller matrix ellipsometer, where P and A are polarizers and Q_G and Q_A are quarter-wave retarders. (a) Optical setup for measuring the polarization properties of the first-order transmitted diffraction of the nanostructure with gammadion shape. (b) Optical setup for measuring the polarization properties of the first-order reflected diffraction of the nanostructure with gammadion shape.

of first-order diffraction is contributed by LD and CB, and the change of ellipticity angle is caused by CD and LB. Through this study, the weighting of LB, CB, LD, and CD is demonstrated.

Results

Three types of gammadion-shaped metasurfaces (GMSs) with different branches and metal thicknesses are fabricated and simulated. The objective of modifying these physical parameters of the GMS (number of branches and metal thickness) is to investigate the influence of these parameters on the type of optical anisotropy produced. The physical parameters of the fabricated gammadion-shaped nanostructures are shown in Table 1 in which the linewidth, the metal thickness, and the number of branches are considered.

The scanning electron microscopy (SEM) image of the two-branch gammadion-shaped nanostructures G215 and the three-branch G315 are illustrated in Fig. 1(a,b), respectively.

For the experimental arrangement, we used a Mueller matrix ellipsometer to study the polarization properties of the gammadion-shaped nanostructure. A frequency-stabilized He-Ne laser (R-32734 Newport, Irvine, CA, United States) was used as the light source for the Mueller matrix ellipsometer, whose central wavelength at 632.8 nm was incident on the sample (Fig. 2) in the transmission mode and reflection mode.

The polarization transfer function of the first-order transmitted diffraction under the normal incidence describes the transmission properties of the gammadion-shaped metasurface. Additionally, the reflection properties are used to characterize the first-order reflected diffraction light with oblique incidence at an incident angle of

	First-order transmitted diffraction		
	G315	G215	G218
D_H	0.041 ± 0.000	0.119 ± 0.002	0.005 ± 0.002
D_{45}	0.338 ± 0.001	0.601 ± 0.005	0.416 ± 0.002
D_C	0.055 ± 0.002	-0.008 ± 0.001	-0.027 ± 0.003
Φ (deg)	0.348 ± 0.055	-0.641 ± 0.059	0.623 ± 0.141
Γ (deg)	91.934 ± 0.282	78.133 ± 0.188	48.503 ± 0.277
ψ (deg)	-46.350 ± 0.035	-51.951 ± 0.064	-47.995 ± 0.140
Δ	0.026 ± 0.002	0.014 ± 0.006	0.066 ± 0.003

Table 2. Polarization properties of the gammadion-shaped nanostructures under the transmission measurements.

	First-order reflected diffraction		
	G315	G215	G218
D_H	0.157 ± 0.021	0.360 ± 0.012	0.059 ± 0.006
D_{45}	-0.137 ± 0.013	-0.015 ± 0.001	-0.086 ± 0.007
D_C	-0.241 ± 0.003	-0.013 ± 0.007	-0.011 ± 0.001
Φ (deg)	-27.795 ± 0.755	-46.500 ± 0.448	-62.903 ± 0.517
Γ (deg)	73.278 ± 0.982	76.522 ± 0.326	109.796 ± 0.148
ψ (deg)	63.226 ± 0.307	62.961 ± 0.312	59.561 ± 0.203
Δ	0.245 ± 0.006	0.285 ± 0.005	0.166 ± 0.001

Table 3. Polarization properties of the gammadion-shaped nanostructures under the reflection measurements.

70°. The measured Mueller matrix (shown in the supplementary information) is decomposed into three Mueller matrices using polar decomposition¹¹. Furthermore, the polarization properties, including LD, CD, LB, CB, and depolarization, are calculated from the decomposed Mueller matrices. The results for transmission and reflection modes are listed in Tables 2 and 3.

According to the measured result from Table 2, for the transmission mode, all tested samples are weak-depolarizing (see row Δ). For D_{45} , the nanostructures express the strongest diattenuation in the $+45^\circ/-45^\circ$ direction. However, the horizontal diattenuation D_H and circular diattenuation D_C are at least fivefold weaker than D_{45} . Thus, the effect from D_H and D_C could be neglected. For retardation (see the rows of linear phase retardation Γ , fast axis orientation ψ , and circular phase retardation Φ), the fast axis of the linear phase retarder is close to -45° , and the circular phase retardation is close to zero. As a result, when the incident light is normal-incident upon a gammadion-shaped structure, the polarization conversion from the incident light to the first diffracted light exhibits linear-amplitude and linear-phase anisotropies, and the principal axes of the linear-amplitude and linear-phase anisotropies nearly coincide.

For the reflection mode, shown in Table 3, the polarization properties of the first-order reflected diffraction of the measured gammadion metasurface exhibit the following characteristics: (1) the depolarization is stronger than that of the transmitted mode. (2) The linear anisotropy is stronger than the circular anisotropy, which implies that Γ is larger than Φ , and the linear diattenuation, defined as $D_L = \sqrt{D_H^2 + D_{45}^2}$, is also either nearly equal to or larger than the circular diattenuation D_C .

A computer simulation is also used to predict the emergent polarization state of the first-order diffracted light transmitted from the gammadion-shaped metasurface when a series of linearly polarized light with different azimuth angles is incident upon the surface. In Figs 3, 4 and 5, the red dots are the results simulated by CST software (Computer Simulation Technology, Framingham, MA, United States), and the black dots are the experimental results, which are obtained by the following steps. An experimental Stokes vector of the emergent polarization state is obtained by multiplying the experimental Mueller matrix of the tested specimen with an ideal incident polarization state; thus, the azimuth angle θ and ellipticity angle ε are obtained from equations (1) and (2):

$$\theta = \frac{1}{2} \tan^{-1} \left(\frac{S_2}{S_1} \right), \quad (1)$$

and

$$\varepsilon = \frac{1}{2} \sin^{-1} \left(\frac{S_3}{\sqrt{S_1^2 + S_2^2 + S_3^2}} \right). \quad (2)$$

where S_i ($i = 0, 1, 2, 3$) are the elements of the Stokes vector. A comparison of the experimental results with the simulated results indicates that our experimental results correspond well with the theoretical predictions. In

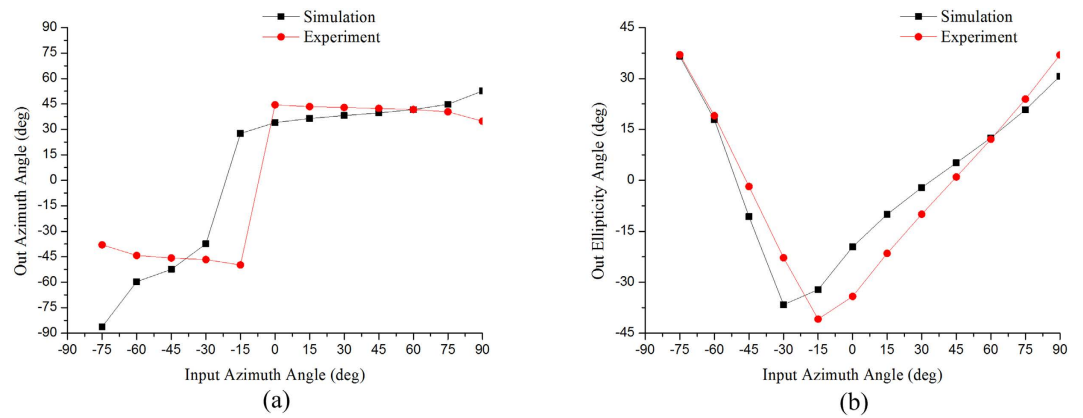


Figure 3. (a) Azimuth angle and (b) ellipticity angle of the output polarization state of the first-order diffracted light transmitted from the G315 nanostructure with a gammadion shape under different input linear polarization states. The red dots are the experimental results, and the black dots are the simulated results.

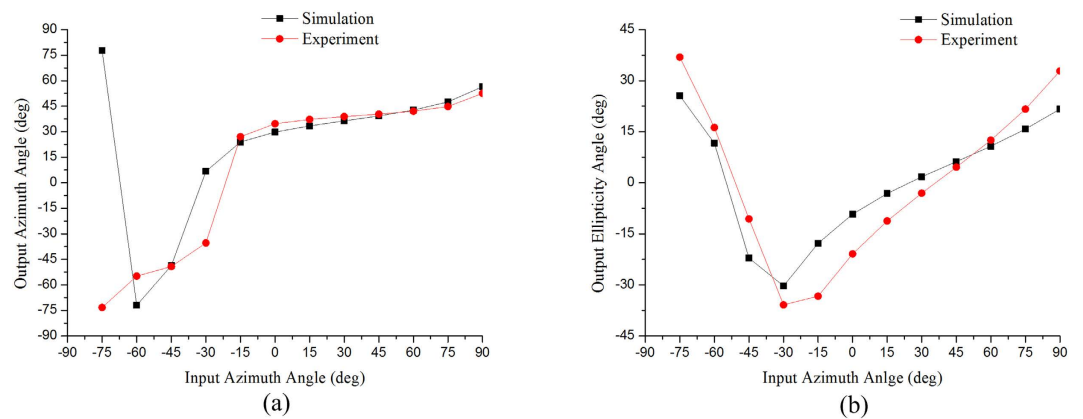


Figure 4. (a) Azimuth angle and (b) ellipticity angle of the output polarization state of the first-order diffracted light transmitted from the G215 nanostructure with a gammadion shape under different input linear polarization states. The red dots are the experimental results, and the black dots are the simulated results.

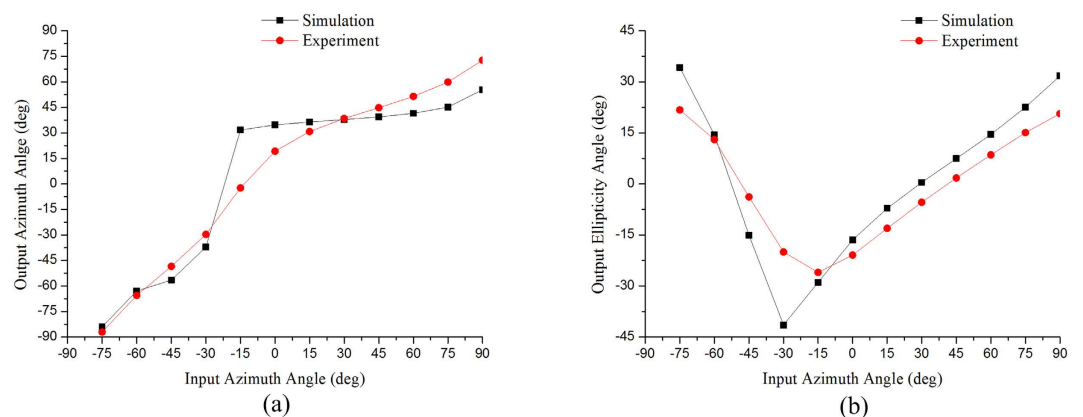


Figure 5. (a) Azimuth angle and (b) ellipticity angle of the output polarization state of the first-order diffracted light transmitted from the G218 nanostructure with a gammadion shape under different input linear polarization states. The red dots are the experimental results, and the black dots are the simulated results.

accordance with Table 2, the principal axes of the measured metasurfaces are close to $+45^\circ/-45^\circ$. In other words, we can deduce the eigen-polarization states of the gammadion-shaped metasurface are $+45^\circ$ and -45° linearly

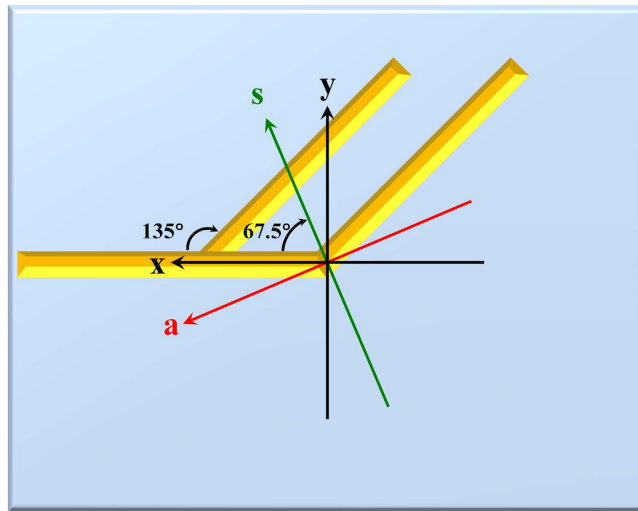


Figure 6. The symmetry axis (**s**) and asymmetry axis (**a**) of the branch of the gammadion-shaped metasurface.

polarized light (see Figs 3–5). This investigation provides strong evidence that the eigen-polarization state is a pair of the mutually and nearly linear polarization states. Because the polarization property of the first-order transmitted diffraction of these metasurfaces is similar to purely linear anisotropy, the azimuth angle change results from the linear amplitude anisotropy (LD) and the ellipticity angle change results from the linear phase anisotropy (LB). This observation is in contrast to previously proposed explanations.

Discussion

The measured results indicate that the optical rotation induced by an artificial chiral nanostructure is not simply a CB component. In our experiment, the contribution of the polarization-conversion effect from the circular phase and the amplitude anisotropies is lower than found in previous research. By using the Mueller matrix ellipsometer, one can investigate the polarization properties (depolarization, diattenuation, and retardation) through the output light that passes through an undetermined material. In this study, the polarization properties of the first-order transmitted diffraction of a gammadion-shaped metasurface are dominated by linear anisotropy and have weak depolarization. Moreover, the polarization properties of the first-order reflected diffraction of a gammadion-shaped metasurface exhibits both linear and circular anisotropies and has stronger depolarization.

The contribution of the linear anisotropy and circular anisotropy of the polarization properties in the first-order transmitted diffraction and first-order reflected diffraction of the GMS might result from the geometry of the gammadion-shaped nanostructure. In transmission mode, we conclude that the polarization rotation effect results from the linear diattenuation, and the change in the ellipticity results from the linear phase retardation. In reflection mode, the polarization rotation effect results from the synergy of linear diattenuation and circular birefringence, and the change in the ellipticity results from the synergy of the circular diattenuation and linear birefringence.

This gammadion-shaped structure can be decomposed into two parts: the cross and the branches. The induced optical anisotropy of the GMS might be explained according to the research on V-shaped nanostructures^{15–17}, in first-order transmitted diffraction, the branches and the cross can be treated as the V-shaped nanostructure with different included angles. We could deduce that the linear phase retardation results from the parts of the included angle between the branches and the cross. According to the articles published by Yu *et al.*¹⁵, the included angle of the V-shaped nanostructure is related to the linear phase retardation. They discussed the reason for linear phase retardation using generalized laws of reflection and refraction derived from Fermat's principle¹⁵. Thus, the angle between the branch and the cross results in the change in the ellipticity. Moreover, the metal branches and cross could contribute to the linear diattenuation, which could result in the polarization rotation. Thus, the polarization effect of the metal branches and cross could be recognized as a metal grid. Similar to the wire-grid partial polarizer¹⁸, the cross portion of the metal layer generates the surface current along the x- and y-directions equally so that the net effect is the induction of the 45°-linear diattenuation. The branches are oriented at 45° and –45°, and they contribute to the linear diattenuation.

In first-order reflected diffraction, the linear anisotropy might result from the contribution of the branches. The branches can be treated as a V-shape nanostructure, in theory, the symmetry axis of the branches of the designed GMS is equal to 67.5° (Fig. 6), which is in contrast to the experimental results in which the fast axis is close to the symmetry axis of the branch as well as the V-shaped nanostructure. Additionally, circular anisotropy is only observed in the reflection but not in the transmission. This is because the oblique incidence has in plane and out of plane polarized components; however, the normal incidence only possesses the in plane polarized component. We suggest that the in plane excitation may contribute to the linear anisotropy, while the out of plane may contribute to the circular anisotropy.

In the near future, we will use the Mueller matrix ellipsometer and the polar-decomposition method to study the polarization properties of other nanostructures.

Methods

Preparation of the gammadion-shaped metasurface. An E-beam writer (Elionix, ELS-7800) is used to draw the gammadion-shaped pattern. Indium tin oxide (ITO) is deposited with a thickness of 3 nm on a glass slide (1 cm × 1 cm). Then, a photoresist spinner (MS-A100, Mikasa, Tokyo, Japan) is used to coat photoresist (PMMA950) on the substrate, which is placed on a hot plate (HP-11 LA, Askul, Tokyo, Japan) for gentle heating for 90 s at 200 °C. After the E-beam process, the slide is immersed in a 1:3 methyl isobutyl ketone (MIBK): isopropyl alcohol (IPA) developer solution for 1 min and then in IPA for 20 s. To deposit the metal onto the glass, we placed the glass slide in an E-gun evaporator (Fulintec, FU-PEB-500). First, we deposited a Ti thin film with a thickness of 5 nm as an adhesive layer, and then, we deposited gold with a thickness of 50 nm and 80 nm. Note that the deposition rate is controlled at 0.5 Å/s. In the lift-off process, we placed the deposited glass slide in acetone and gently agitated the beaker. When the gold film on the photoresist was lifted off, the sample preparation for measurement was complete.

Computer simulation. To simulate the gammadion-shaped metasurfaces, we used commercial finite element-based electromagnetic field solver (CST Microwave Studio™) and calculated the polarization rotation and ellipticity in first order transmitted diffraction light. Two types of complex gammadion-shaped structures were designed and simulated. The bottom substrate is porous silica, and a 5-nm thick indium tin oxide (ITO) layer lies on top of the silica. The corrugated metallic gammadion arrays consist of 5 nm Ti as the adhesive layer and 50 nm and 80 nm gold film. Then, these gammadion-shaped metasurfaces were illuminated by a linearly polarized plane wave with a wavelength of 632.8 nm and with a periodic boundary condition. The azimuth angle of the incident linear polarization state was varied from 0° to 180°, and the interval of the simulated point was 15°. The refractive index of the glass is 1.5, and the material properties of ITO, Ti and Au are based on ref. [19], ref. [20] and ref. [20], respectively. In the simulation, the polarization rotation azimuth angle and the ellipticity angle were calculated using the Stokes parameter for different types of structures.

Characterization of the polarization properties of a gammadion-shaped metasurface.

Theoretically, the ensemble polarization conversion from a photonic device or material is caused by optical anisotropy. Optical anisotropy includes linear amplitude anisotropy, linear phase anisotropy, circular amplitude anisotropy, and circular phase anisotropy. The polarization transfer function directly reflects the polarization characteristics for an unknown optical system or the optical components. In this study, we analyze the amplitude and phase anisotropies of the gammadion-shaped nanostructure in terms of the Mueller calculus. The relation between light and the optical system can be represented as $S_o = MS_i$ or

$$\begin{pmatrix} S_0^{out} \\ S_1^{out} \\ S_2^{out} \\ S_3^{out} \end{pmatrix} = \begin{pmatrix} m_{11} & m_{12} & m_{13} & m_{14} \\ m_{21} & m_{22} & m_{23} & m_{24} \\ m_{31} & m_{32} & m_{33} & m_{34} \\ m_{41} & m_{42} & m_{43} & m_{44} \end{pmatrix} \begin{pmatrix} S_0^{in} \\ S_1^{in} \\ S_2^{in} \\ S_3^{in} \end{pmatrix}. \quad (3)$$

where S_o and S_i are the Stokes vectors of the output and input light, respectively, and M is the Mueller matrix for an arbitrary optical system. According to the method proposed by Lu and Chipman, the Mueller matrix of an undetermined specimen can be divided into three matrices¹¹:

$$M = M_{\Delta} M_R M_D. \quad (4)$$

where M_{Δ} , M_R , and M_D are the Mueller matrices for depolarization, phase retardation, and diattenuation, respectively. Matrix M can be decomposed into these three matrices according to polar decomposition, which is described in ref. 10 in detail. In equation (4), M_D describes the polarization-dependent transmission of the undetermined specimen. The polarization properties of a diattenuator can be characterized by three diattenuations, which are the horizontal diattenuation, D_H , 45°-linear diattenuation, D_{45} , and circular diattenuation, D_C , defined as

$$D_H = \frac{T_H - T_V}{T_H + T_V}, \quad D_{45} = \frac{T_{+45} - T_{-45}}{T_{+45} + T_{-45}}, \quad \text{and} \quad D_C = \frac{T_R - T_L}{T_R + T_L}. \quad (5)$$

where T is the transmittance and the subscripts H, V, +45, −45, R, and L denote horizontally, vertically, +45° linearly, −45° linearly, right-handed circularly, and left-handed circularly polarized light, respectively. These three diattenuations indicate the amplitude anisotropy of the specimen. M_{Δ} describes the capability of depolarization by the undetermined specimen, which can depolarize the incident polarization state. Furthermore, the diagonal matrix elements of M_{Δ} : $m_{\Delta 22}$, $m_{\Delta 33}$, and $m_{\Delta 44}$ indicate the depolarization coefficients for depolarizing the incident horizontal, 45° linear, and circular polarization states, respectively. The net depolarization power of the undetermined specimen is determined by the parameter Δ , which can be obtained from

$$\Delta = 1 - \frac{|\text{tr}(M_{\Delta}) - 1|}{3}, \quad 0 \leq \Delta \leq 1. \quad (6)$$

where $\text{tr}(M_{\Delta})$ is the trace of M_{Δ} . A specimen is completely depolarizing when Δ approaches 1. In theory, M_R can be further decomposed into a linear phase retarder M_{LR} and a circular phase retarder M_{CR} . M_{LR} would follow M_{CR} , such as $M_R = M_{CR} M_{LR}$. For M_R , the corresponding parameters are Γ , ψ , and Φ , which represent the linear

phase retardation, fast-axis angle, and circular phase retardation, respectively. These three parameters can express the phase anisotropy. Theoretically, once \mathbf{M}_R is obtained, the parameters Γ , ψ , and Φ can be calculated from equations (7), (8), and (9), respectively.

$$\Gamma = \cos^{-1}[\sqrt{(m_{R22} + m_{R33})^2 + (m_{R32} - m_{R23})^2} - 1], \quad (7)$$

$$\psi = \frac{1}{2} \tan^{-1}\left(\frac{m_{R42}}{-m_{R43}}\right), \quad (8)$$

and

$$\Phi = \frac{1}{2} \tan^{-1}\left(\frac{m_{R32} - m_{R23}}{m_{R22} + m_{R33}}\right). \quad (9)$$

where m_{Rij} ($i, j = 1, 2, 3, 4$) are the Mueller matrix elements of \mathbf{M}_R .

Measurement of the Mueller matrix ellipsometer. Mueller matrix ellipsometry and Fourier analysis are combined to measure the 15 normalized Mueller matrix elements of a gammadion-shaped metasurface (normalized by m_{11} ; see eq. (3))²¹. We utilize the Mueller matrix ellipsometer illustrated in Fig. 2(a,b) to measure the Mueller matrix of the transmission and reflection properties of the gammadion-shaped metasurface, respectively. In Fig. 2, P and A are the polarizer and analyzer, and their transmission axes are preset to be parallel to the x-axis. Q_G and Q_A are the quarter-wave retarders whose fast axes are also preset to be parallel to the x-axis. Then, Q_G and Q_A rotate simultaneously by the motorized rotation stages, and the ratio of the angular speeds is 5:1¹⁰. Thus, we have

$$Q_G = \omega t, \quad Q_A = 5\omega t \quad (10)$$

The time-varying intensity signal $I(t)$ is received by the photodetector, and this signal has fundamental and harmonic components¹⁰. According to Fourier theory, we can decompose $I(t)$ into cosine series and sine series, such as

$$I(t) = a_0 + \sum_{n=1}^{12} a_n \cos 2n\omega t + b_n \sin 2n\omega t \quad (11)$$

According to equation (11), the Fourier amplitudes a_0 , a_n , and b_n ($n = 1, 2, 3, \dots$) can be obtained by Fourier analysis. These Fourier amplitudes are a function of the Mueller matrix elements ($m_{11}, m_{12}, \dots, m_{44}$), which is described in Table 1 of ref. 10. Thus, we can obtain the Mueller matrix elements from the Mueller matrix ellipsometer.

References

- Pendry, J. B. Negative refraction makes a perfect lens. *Phys. Rev. Lett.* **85**, 3966–3969 (2000).
- Yen, T. J. *et al.* Terahertz magnetic response from artificial materials. *Science* **303**, 1494–1496 (2004).
- Smith, D. R., Pendry, J. B. & Wiltshire, M. C. K. Metamaterials and negative refractive index. *Science* **305**, 788–792 (2004).
- Bai, B., Laukkanen, J., Lehmuskero, A. & Turunen, J. Simultaneously enhanced transmission and artificial optical activity in gold film perforated with chiral hole array. *Phys. Rev. B* **81**, 115424 (2010).
- Papakostas, A. *et al.* Optical manifestations of planar chirality. *Phys. Rev. Lett.* **90**, 107404 (2003).
- Li, Z., Mutlu, M. & Ozbay, E. Chiral metamaterial: from optical activity and negative index to asymmetric transmission. *J. Opt.* **15**, 023001 (2013).
- Yariv, A. & Yeh, P. *Optical Waves in Crystals* (Wiley, 1984).
- Lin, C., Yu, C., Chen, C., Chou, L. & Chou, C. Kinetics of glucose mutarotation assessed by an equal-amplitude paired polarized heterodyne polarimeter. *J. Phys. Chem. A* **114**, 1665–1669 (2010).
- Schellman, J. A. Circular dichroism and optical rotation. *Chem. Rev.* **75**, 323–331 (1975).
- Azzam, R. M. A. Photopolarimetric measurement of the Mueller matrix by Fourier analysis of a single detected signal. *Opt. Lett.* **2**, 148–150 (1978).
- Lu, S. & Chipman, R. A. Interpretation of Mueller matrices based on polar decomposition. *J. Opt. Soc. Am. A* **13**, 1106–1113 (1996).
- Yu, C. J., Lin, C. E., Su, L. C. & Chou, C. Heterodyne linear polarization modulation ellipsometer. *Jan. J. Appl. Phys.* **48**, 032403 (2009).
- Oates, T. W. H., Wormeester, H. & Arwin, H. Characterization of plasmonic effects in thin films and metamaterials using spectroscopic ellipsometry. *Prog. Surf. Sci.* **86**, 328–376 (2011).
- Jones, R. C. A new calculus for the treatment of optical systems I. Description and discussion of the calculus. *J. Opt. Soc. Am.* **31**, 488–493 (1941).
- Yu, N. *et al.* Light propagation with phase discontinuities: generalized laws of reflection and refraction. *Science* **334**, 333–337 (2011).
- Yin, X., Ye, Z., Rho, J., Wang, Y. & Zhang, X. Photonic spin hall effect at metasurfaces. *Science* **339**, 1405–1407 (2013).
- Yu, N. *et al.* A broadband, background-free quarter-wave plate based on plasmonic metasurfaces. *Nano Lett.* **12**, 6328–6333 (2012).
- Hecht, E. *Optics*, 4th edn, 333–334 (Addison-Wesley, 2002).
- Laux, S. *et al.* Room-temperature deposition of indium tin oxide thin films with plasma ion-assisted Evaporation. *Thin Solid Films* **335**, 1 (1998).
- Palik, E. D. *Handbook of Optical Constants of Solids* (Academic Press, 1985).
- Manhas, S. *et al.* Mueller matrix approach for determination of optical rotation in chiral turbid media in backscattering geometry. *Opt. Express* **14**, 190–202 (2006).

Author Contributions

C.E.L. and C.J.Y. performed the experimental setup and fabricated the gammadion-shaped metamaterial. C.J.Y. designed the Mueller matrix ellipsometer and developed the theoretical modeling. T.J.Y. and C.W.C. proposed the optimal parameter for fabricating the nanostructure. C.M.H. performed the data acquisition. M.H.L. used CST for the simulation of the gammadion-shaped nanostructure. C.E.L., C.J.Y. and C.C.C. calculated and analysis the polarization properties of the gammadion-shaped metasurface. C.E.L. *et al.* discussed the experimental data, analytical developments and simulation results and wrote the paper.

Additional Information

Supplementary information accompanies this paper at <http://www.nature.com/srep>

Competing financial interests: The authors declare no competing financial interests.

How to cite this article: Lin, C.-E. *et al.* Singular observation of the polarization-conversion effect for a gammadion-shaped metasurface. *Sci. Rep.* **6**, 22196; doi: 10.1038/srep22196 (2016).



This work is licensed under a Creative Commons Attribution 4.0 International License. The images or other third party material in this article are included in the article's Creative Commons license, unless indicated otherwise in the credit line; if the material is not included under the Creative Commons license, users will need to obtain permission from the license holder to reproduce the material. To view a copy of this license, visit <http://creativecommons.org/licenses/by/4.0/>